Improvement of the GERDA ge detectors energy resolution by an optimized digital signal processing

Benato, G ; D'Andrea, V ; Cattadori, C ; Riboldi, S

Abstract: The GERmanium Detector Array (Gerda) at the Gran Sasso Underground Laboratory (LNGS) searches for the neutrinoless double beta decay (0) of76 Ge. Germanium detectors made of material with an enriched76 Ge fraction act simultaneously as sources and detectors for this decay. During Phase I of theexperiment mainly refurbished semi-coaxial Ge detectors from former experiments were used. For the upcoming Phase II, 30 new76 Ge enriched detectors of broad energy germanium (BEGe)-type were produced. A subgroup of these detectors has already been deployed in Gerda during Phase I. The present paper reviews the complete production chain of these BEGe detectors including isotopic enrichment, purification, crystal growth and diode production. The efforts in optimizing the mass yield and in minimizing the exposure of the76 Ge enriched germanium to cosmic radiation during processing are described. Furthermore, characterization measurements in vacuum cryostats of the first subgroup of seven BEGe detectors and their long-term behavior in liquid argon are discussed. The detector performance fulfills the requirements needed for the physics goals of Gerda Phase II.

DOI: https://doi.org/10.1016/j.phpro.2014.12.069

Available online at www.sciencedirect.com

ScienceDirect

Physics Procedia 61 (2015) 673 – 682

Physics Procedia

13th International Conference on Topics in Astroparticle and Underground Physics

Improvement of the GERDA Ge Detectors Energy Resolution by an Optimized Digital Signal Processing

G. Benato[a,*], V. D'Andrea[b], C. Cattadori[c,d], S. Riboldi[e]

[a] *Physik Institut der Universität Zürich, Zürich, Switzerland*
[b] *Gran Sasso Science Institute, L'Aquila, Italy*
[c] *Università di Milano Bicocca, Milano, Italy*
[d] *INFN Milano Bicocca, Milano, Italy*
[e] *Università degli studi di Milano e INFN Milano, Milano, Italy*

Abstract

GERDA is a new generation experiment searching for neutrinoless double beta decay of ^{76}Ge, operating at INFN Gran Sasso Laboratories (LNGS) since 2010. Coaxial and Broad Energy Germanium (BEGe) Detectors have been operated in liquid argon (LAr) in GERDA Phase I. In the framework of the second GERDA experimental phase, both the contacting technique, the connection to and the location of the front end readout devices are novel compared to those previously adopted, and several tests have been performed.

In this work, starting from considerations on the energy scale stability of the GERDA Phase I calibrations and physics data sets, an optimized pulse filtering method has been developed and applied to the Phase II pilot tests data sets, and to few GERDA Phase I data sets. In this contribution the detector performances in term of energy resolution and time stability are here presented.

The improvement of the energy resolution, compared to standard Gaussian shaping adopted for Phase I data analysis, is discussed and related to the optimized noise filtering capability. The result is an energy resolution better than 0.1% at 2.6 MeV for the BEGe detectors operated in the Phase II pilot tests and an improvement of the energy resolution in LAr of about 8% achieved on the GERDA Phase I calibration runs, compared to previous analysis algorithms.

Selection and peer review is the responsibility of the Conference lead organizers, Frank Avignone, University of South Carolina, and Wick Haxton, University of California, Berkeley, and Lawrence Berkeley Laboratory

Keywords: neutrinoless double beta decay, digital signal processing.
PACS: 07.05.kf, 23.40-s

1. Introduction

The GERmanium Detector Array (GERDA) experiment [1], located at the underground Gran Sasso Laboratory of INFN (Italy), is devoted to the study of neutrinoless double-beta decay ($0\nu\beta\beta$) of ^{76}Ge with a large mass of germanium detectors isotopically enriched in ^{76}Ge.

*Corresponding author
Email address: gbenato@physik.uzh.ch (G. Benato)

Selection and peer review is the responsibility of the Conference lead organizers, Frank Avignone, University of South Carolina, and Wick Haxton, University of California, Berkeley, and Lawrence Berkeley Laboratory
doi:10.1016/j.phpro.2014.12.069

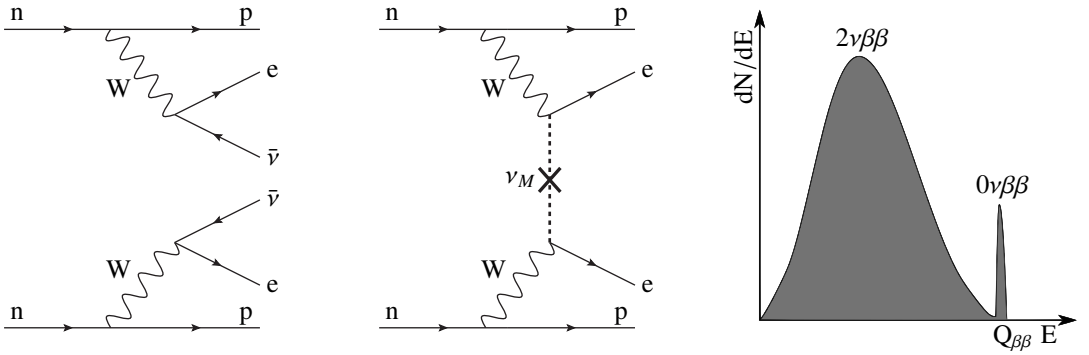

Fig. 1: In the $2\nu2\beta$ decay final state (left) the available energy is divided among the four outgoing particles. On the other side, in $0\nu\beta\beta$ decay it is divided only between the two electrons (middle). As a consequence, the sum spectrum of the two electrons will be a continuum from zero to $Q_{\beta\beta}$ for the $2\nu\beta\beta$ decay, and, neglecting the nuclear recoil, a peak at $Q_{\beta\beta}$ for the $0\nu\beta\beta$ decay (right).

The $0\nu\beta\beta$ process is forbidden by the Standard Model (SM) because it violates the lepton number conservation by two units. It is different from the two neutrino double-beta decay ($2\nu\beta\beta$), allowed by the SM, in the final state (Fig. 1). The observation of the $0\nu\beta\beta$ would have important consequences in astroparticle physics: it would prove that neutrinos have a Majorana mass component and, assuming the exchange of light Majorana neutrinos, an effective neutrino mass could be evaluated by using predictions for the nuclear matrix element (NME).

The experimental signature of $0\nu\beta\beta$ decay is a peak in the two electrons sum spectrum at the Q-value of the decay ($Q_{\beta\beta}$, 2039 keV for ^{76}Ge). Still now there is no aknowledged evidence of the existence of this decay [2]. For ^{76}Ge, the most recent results were published by the GERDA collaboration [3], with a new limit for the half-life of the process of $T^{0\nu}_{1/2} > 2.1 \cdot 10^{25}$ yr (90% CL).

To be competitive with the published half-life limits [3][4][5], an up-to-date Ge experiment should expose a mass M of 10^{26}-10^{27} candidate nuclei, for an exposure t of O(years), with a background index (BI) of $\sim 10^{-3}$ counts/(keV·kg·yr), a FWHM at $Q_{\beta\beta}$ of $O(0.1\%)$, and a total efficiency (ε) of $O(90\%)$. The achievable limit on $T^{0\nu}_{1/2}$ at a given confidence level n_σ can be expressed as:

$$T^{0\nu}_{1/2} = \frac{\ln 2 \cdot N_A}{n_\sigma \sqrt{2}} \frac{a \cdot \varepsilon}{A} \sqrt{\frac{M \cdot t}{BI \cdot \Delta E}} \tag{1}$$

where a is the enrichment fraction of the source (for ^{76}Ge, $a \geq 86\%$ with the present technology), and $\sqrt{2}$ comes from the assumption of having the same number of signal and background counts. The energy resolution ΔE, *i.e.* as the Full Width at Half Maximum (FWHM) of an hypothetical gamma line at $Q_{\beta\beta}$, plays a major role in the final analysis. An improved resolution means higher sensitivity to the presence of signal- or background-induced gamma peaks and increased sensitivity in the construction of the background model. In GERDA, due to the use of germanium detectors, the mass averaged FWHM at $Q_{\beta\beta}$ is 2.4‰ and 1.6‰ for coaxial and BEGe detectors, respectively [3]. Despite this is one of the best energy resolution achieved in the field, a further improvement can be obtained by using an optimized technique for the offline energy evaluation.

The detectors of GERDA are mounted on low-mass copper supports and immersed in a 64 m^3 cryostat filled with liquid argon (LAr). The LAr serves at the same time as cooling medium and shield against external background radiation. The shielding is complemented by a 3 m thick water tank, instrumented with photo multipliers to detect Cherenkov light generated by muons. A graphical description of the experimental setup is given in Fig. 2.

The first phase of the experiment, denoted as GERDA Phase I and operative between November 2011 and June 2013, used reprocessed p-type semi-coaxial detectors from the HDM [6] and IGEX [7] experiments.

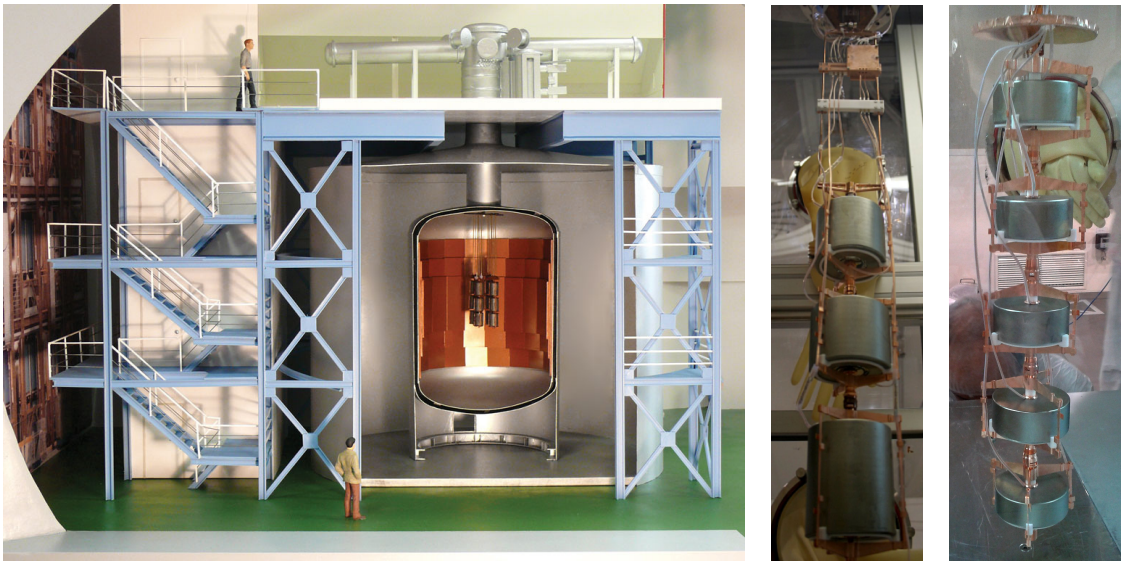

Fig. 2: Left: a mock-up of GERDA, with the water tank, the cryostat and, in the center, the detectors (not in scale). Middle: a string with three coaxial detectors prior to the installation in GERDA. Right: the first five BEGe detectors being installed in GERDA during Phase I data acquisition.

Phase II will operate about 30 Broad Energy Germanium detectors (BEGe), enriched in ^{76}Ge, manufactured by Canberra [8] and fully characterized in vacuum cryostat soon after their production [9]. This paper reports the data processing results from some BEGes tests and also from the reprocessing of some GERDA Phase I calibration runs, both with semi-coaxial and BEGe detectors.

2. Digital Signal Processing in the GERDA Experiment

The current energy reconstruction in GERDA is performed via an offline analysis of the digitized charge pulses performed with the software tool GELATIO [10], in which a standard semi-Gaussian shaping is implemented. Events generated by discharges or due to electromagnetic noise are rejected by a set of quality cuts, as well as coincidences and pile-up events.

The digital semi-Gaussian shaping used in GERDA consists of two operations:

- a differentiation of the sampled signal $x_0[t]$ with time delay $L = 5\ \mu s$:

$$x_0[t] \rightarrow x_1[t] = x_0[t] - x_0[t - L] \tag{2}$$

- a Moving Average (MA) with the same width, repeated 25 times:

$$x_i[t] \rightarrow x_{i+1}[t] = \frac{1}{L} \sum_{t'=t-L}^{t} x_i[t'] \quad \text{with} \quad i = 1 \dots 25 \tag{3}$$

The energy is then given by the height of the shaped signal. This algorithm is stable and relatively fast, but it is limited by several factors, as described in detail in Sec. 3.2. A graphical description of the semi-Gaussian shaping is reported in Fig. 3.

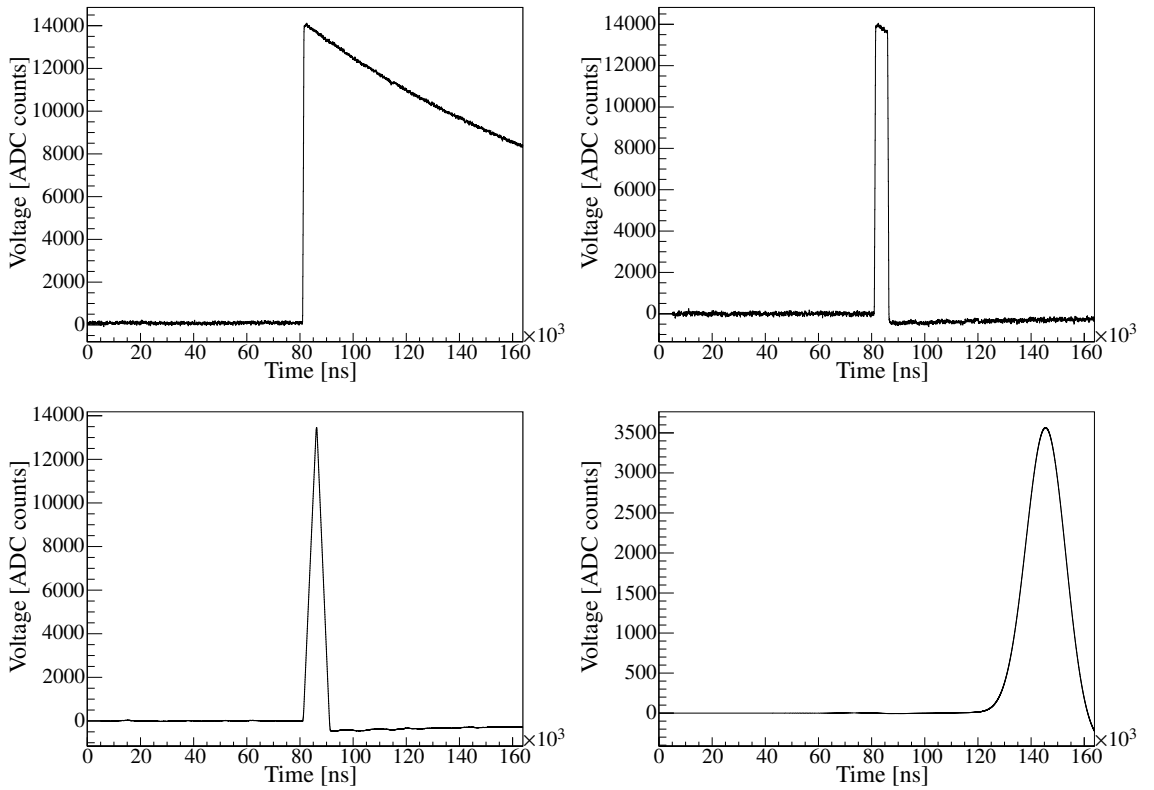

Fig. 3: Top left: typical waveform recorded in GERDA Phase I. Top right: the waveform after the differentiation operation described in Eq. 2. Bottom: the signal after one (left) and 25 (right) moving average operations (see Eq. 3).

3. Development of a New Filter Algorithm for the Energy Evaluation in GERDA

3.1. Energy Resolution and Noise Components

The resolution of a germanium detector can be expressed by the full with at half maximum (FWHM) of a reference gamma line in the energy spectrum as:

$$\mathrm{FWHM}^2 = \mathrm{FWHM}^2_{\mathrm{det}} + \mathrm{FWHM}^2_{\mathrm{charge}} + \mathrm{FWHM}^2_{\mathrm{noise}} \tag{4}$$

where:

- $\mathrm{FWHM}_{\mathrm{det}} = 2.35\sqrt{\varepsilon \cdot \mathrm{F} \cdot \mathrm{E}}$ is the intrinsic detector's resolution, representing the charge fluctuation ($\mathrm{F} \simeq 0.13$ is the Fano factor and $\varepsilon = 2.96$ eV is the ionization energy of germanium at liquid nitrogen temperature);
- $\mathrm{FWHM}_{\mathrm{charge}}$ is connected to the incomplete charge collection. This term is negligible if the high voltage (HV) applied to the diode is enough to ensure a full depletion. For the case of GERDA Phase I, the high leakage current on three detectors could only be solved by reducing the HV (and eventually turning them off completely), thus leading to a very poor energy resolution;
- $\mathrm{FWHM}_{\mathrm{noise}}$ is the electronic noise induced by the electrical components connected to the detector, by the noise sources intrinsically related to the detector itself (capacitance, leakage current), and by the electro-magnetic disturbances.

While the $\mathrm{FWHM}_{\mathrm{det}}$ and $\mathrm{FWHM}_{\mathrm{charge}}$ are completely fixed by the experimental setup, $\mathrm{FWHM}_{\mathrm{noise}}$ can be minimized by a proper signal shaping. The equivalent noise charge (ENC) of a generic shaping filter is

characterized by three components: series, 1/f and parallel noise:

$$\mathrm{ENC}^2 = \mathrm{C_T^2}\left(\alpha\frac{v^2}{\sigma_f} + \gamma\mathrm{A}\right) + \beta\sigma_f i^2 \tag{5}$$

where $\mathrm{C_T}$ is the sum between the detector, preamplifier and feedback capacitances, α, β, γ and σ_f are parameters that depends on the filter type, v^2 and i^2 are the root mean values of the series and parallel noise and A is the coefficient of the 1/f noise, *i.e.* characterized by a 1/f behavior in the frequency power spectrum. The optimization of σ_f allows to filter out peculiar noise frequencies and thus to minimize $\mathrm{FWHM_{noise}}$.

3.2. Limits of the Semi-Gaussian Shaping Procedure in GERDA *Phase I*

The semi-Gaussian shaping explained in Sec. 2 acts, through the differentiation, as a high-pass filter followed by n low-pass filters, corresponding to n moving average operations. In particular, it is not specifically reducing 1/f and current low-frequency noise. The resolution obtained with semi-Gaussian shaping is very close to the optimal one if the detectors are operated in standard conditions, *i.e.* in vacuum, with the preamplifier very close to the diode and with short cabling. Unfortunately this is not the case for GERDA Phase I, where the very low background requirements could only be satisfied by installing the preamplifiers at a distance of 0.3-0.8 m from the detectors and by connecting the two with non coaxial Teflon-coated copper strings. In addition, the DAQ system is connected to the front-end electronics through 10 m long resistive coaxial cables. As a consequence, strong low-frequency noise is present in some of the GERDA Phase I detectors [11].

Moreover, the GERDA detectors are characterized by different signal properties and noise conditions. In order to achieve the best possible energy resolution, it is mandatory to tune the shaping filter separately for each channel, which was not done in the first processing of GERDA Phase I data.

Finally, the semi-Gaussian shaping is usually implemented as a chain of one deconvolution and n moving average operations. This could be substituted by a unique convolution with the equivalent filter, thus strongly reducing the computation effort.

3.3. Development of a New Filter Algorithm for the Energy Evaluation in GERDA

The development of a new shaping algorithm for GERDA Phase I was tailored to optimize the FWHM of the gamma lines in the calibration spectra. The performance of the new filter on all Phase I data will be presented in a dedicated paper.

Theoretical studies show that the best noise whitening filter in presence of fundamental voltage series and current parallel noise is the infinite cusp [12]. In practice, given the finite length of the recorded waveforms, the best resolution is obtained using a finite-length cusp filter with the highest length possible, usually approximated as a triangular filter. If additional low frequency noise is present, there is evidence [13] that suitable filters for the subtraction of non-zero baseline and the rejection of low-frequency disturbance can be derived from the finite-length cusp filter by adding a zero total area constraint. A description of the behavior of the triangular filter with and without zero-area condition applied to simulated signals is reported in [14].

When dealing with real signals, the detector properties have to be considered, too, in the creation of an appropriate shaping filter. In particular, the charge collection time for HPGe and BEGe detectors is of order of 1 μs. If this is not taken into account by the filter, ballistic deficit effects become important at high energies, leading to the presence of low-energy tails in the gamma lines of the recorded spectra [15]. The ballistic deficit is minimized by using a constant shaping filter for the duration of charge collection [16]. In digital signal processing (DSP), this is obtained by inserting a flat-top in the central part of the (cusp) filter.

For the case of GERDA, the finite-length cusp filter of length $2L$ and flat-top FT was constructed as:

$$f_{cusp}(t) = \begin{cases} sinh\left(\frac{t}{\sigma_f}\right) & 0 < t < L \\ sinh\left(\frac{L}{\sigma_f}\right) & L < t < L + FT \\ sinh\left(\frac{2L+FT-t}{\sigma_f}\right) & L + FT < t < 2L + FT \end{cases} \tag{6}$$

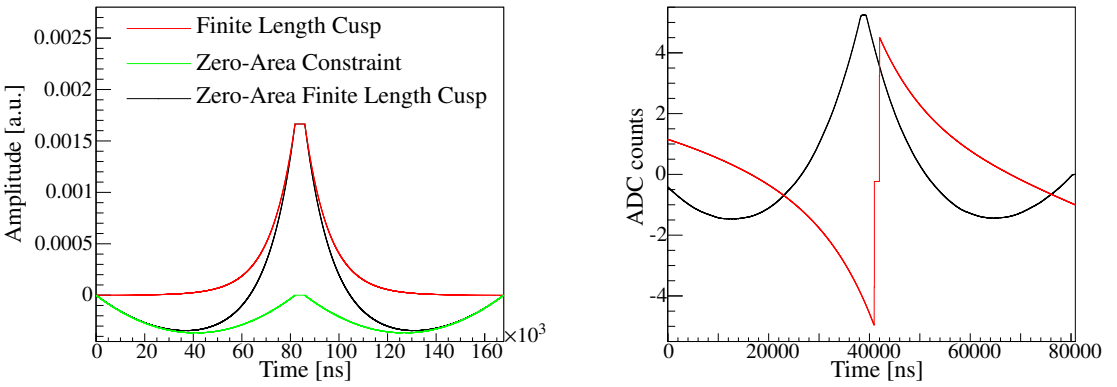

Fig. 4: Left: the ZAC filter (black) is composed by the finite-length cusp (red), to which two parabolas are subtracted on the cusp sides (green). Right: the ZAC filter after the convolution with the inverse preamplifier response function (red) and the waveform of Fig. 3 after the convolution with it.

The zero-area condition was obtained by subtracting two parabolas on the $[0; L]$ and $[L + FT; 2L + FT]$ regions, with total area normalized to that of the cusp filter. The resulting filter is the finite-length zero-area cusp filter (ZAC). A graphical description of the ZAC filter construction is provided in Fig. 4.

Additionally, the preamplifier's effect on the recorded signal has to be accounted for. The response function of a standard charge sensitive preamplifier is an exponential curve, whose decay time is $\tau = 1/\mathrm{RC}$, where R and C are the preamplifier's feedback resistance and capacitance, respectively. The original current pulse, *i.e.* the input pulse of the preamplifier, is obtained via a deconvolution of the recorded waveform with the preamplifier response function, or, in an equivalent way, via a convolution of the recorded waveform with the $H(z) = 1 - az^{-1}$ filter, with the a being a function of τ and the sampling frequency. So far, the correction for the electronics finite bandwidth is not introduced.

The energy estimation is given by the maximum amplitude of the signal obtained through the deconvolution of the preamplifier's response function and the convolution of the current pulse with the ZAC filter. Given the commutative property of the convolution operation, the convolution between the ZAC filter and the preamplifier's inverse response function can be performed once for all, obtaining the filter shown in red in the right panel of Fig. 4, which is then applied to each signal to obtain the output depicted in black. In this way a unique operation is applied to the signals, with a consequent reduction of computation time.

3.4. Optimization of the ZAC Filter for GERDA *Phase I and Phase II Development Tests Data*

The optimization of the ZAC filter for the data collected during GERDA Phase I, as well as for those taken in development test for Phase II, has to be performed on the four filter parameters, L, FT, τ and σ_f.

In principle, the best resolution is obtained by using all the information available in the signal. When dealing with digitized waveforms, this condition corresponds to using the information contained in all the bins. Therefore, the total length of the filter, $2L + FT$, should be equal to the length of the recorded pulse. If the event rate is too high, the presence of pile-up events represents a strong limitation to this procedure. For the case of GERDA, the pile-ups are a background, hence they are rejected. Also in the calibration runs, the sources activity is low enough to limit these events to $\leq 10\%$ of the total, so they can be removed without a major loss of information. On the contrary, a limitation to the use of the longest filter possible for GERDA data is induced by the digital trigger algorithm used, leading to a $\sim$ 1µs variation in the time at which the signal rise takes place. For the analysis of the physics and the calibration data, only the events with a trigger-time contained in a 2 µs window are accepted. As a consequence, the length of the ZAC filter has to be shortened by the same amount.

As mentioned above, the optimal value for FT is connected to the charge collection time. This depends on the detector geometry and electric field, resulting to be $\sim$ 0.7 µs for coaxial and $\sim$ 1 µs for BEGe detectors.

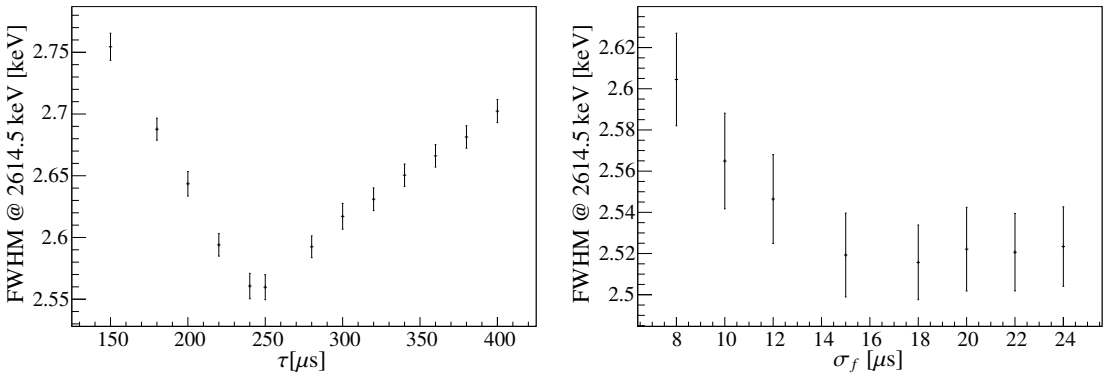

Fig. 5: Optimization of the preamplifier's τ and of the ZAC filter σ_f for the data collected in preparation to GERDA Phase II. The plots are taken from [14].

Moreover, the reconstruction of the original current pulse is achievable only through use of the correct value for the preamplifier's τ. The presence of more preamplifiers on the same base lead to an effective τ, which can be different from what expected by the simple calculation performed on the basis of the used resistance and capacitance. If in principle τ can be estimated using the recorded signals [17], a reasonable result can only be obtained if an enough long ($\sim$ 0.5 ms) decay tail is recorded. Therefore τ is considered here as a free parameter, that has to be optimized. An example is depicted Fig. 5, on the left.

Finally, the optimization of the noise whitening is done by tuning the σ_f parameter, which corresponds to the shaping time of a traditional semi-Gaussian filter. The best resolution is obtained for a value of the shaping time corresponding to the minimum contribution of the parallel and series noise to FWHM_{noise} [18].

Both for the GERDA Phase I and the Phase II preparation test data, the ZAC filter was optimized by using calibration data, collected with ^{228}Th sources [19][20]. In order to reduce the CPU time, the events in a 100 keV range around the ^{208}Tl peak at 2614.5 keV were selected, and different combinations of the filter parameters were used for the reconstruction of the energy spectrum. The high statistics of the ^{208}Tl peak allowed to obtain a precise estimation of the FWHM, with a statistical uncertainty of about 0.02 keV, depending on the specific case. Since the use of a different shaping filter only affects the FWHM_{noise}, the improvement in energy resolution is expected to be constant over all the energy range. In other words, the FWHM at $Q_{\beta\beta}$ should be improved by the same amount as it is at 2614.5 keV.

4. Results

The first positive results were obtained with the data collected in Phase II preparation tests performed in the germanium detector laboratory (GDL), a GERDA test facility at LNGS. A couple of BEGe detectors were operated in standard condition in the GDL test bench, and in LAr in the Liquid Argon Germanium (LArGe) setup [21]. The optimization of the filter was performed in different steps, on the basis of the filter parameters; as an example, the left panel of Fig. 5 shows the result of the optimization of the preamplifier's τ. The spectrum was processed a dozen times with τ varying between 150 and 400 μs, and the best resolution is obtained with $\tau \simeq 145$ μs. The importance of this parameter reveals to be primary, with a very strong dependence of the FWHM on τ. On the right side of Fig. 5, the optimization of σ_f is shown for $\tau =$ 245 μs, where the dependence of the FWHM as function of the shaping time (in our case, σ_f) is clearly reproduced. Also in this case, a wrong choice of the parameter would seriously affect the energy resolution. The best FWHM at 2614.5 keV obtained in the GDL test bench with two detectors was 2.52 ± 0.01 keV, thus equaling the performances obtained with a standard spectroscopic amplifier. For the LArGe measurements, the FWHM was 3.06 ± 0.01 keV, 0.15 keV better than that obtained with the semi-Gaussian shaping. A detailed description of these results is provided in [14].

The ZAC filter was also tested on some GERDA Phase I calibration runs and optimized for each detector separately. In this case the optimization was performed by varying FT, L and σ_f at the same time, thus

Table 1: FWHM at the ^{208}Tl peak obtained with the semi-Gaussian shaping and the optimized ZAC filter, for one typical calibration run. Only the detectors used for the Phase I analysis of $0\nu\beta\beta$ decay are shown. For all the coaxial detectors (ANGs and RGs) the improvement is between 0.2 and 0.5 keV. For the BEGe detectors (last four rows), the improvement is $\sim$ 0.15 keV if no strong low-frequency noise is present. The best results are obtained with Achilles, for which the energy resolution is brought down almost to the level of the other BEGe's thanks to the enhanced low-frequency noise rejection of the ZAC filter.

	FWHM [keV]		
Detector	Semi-Gaussian Shaping	ZAC Shaping	Improvement [keV]
ANG2	4.73	4.29	0.44
ANG3	4.62	4.29	0.33
ANG4	4.41	4.11	0.30
ANG5	4.17	3.87	0.30
RG1	4.67	4.19	0.48
RG2	5.06	4.86	0.20
Agamennone	2.86	2.70	0.16
Andromeda	2.88	2.75	0.13
Anubis	2.91	2.79	0.12
Achilles	3.59	2.85	0.74

producing a full scan of the FWHM over the parameter space. As a proof of the effectiveness of the ZAC filter on low-frequency noise, the FWHM in correspondence of the ^{208}Tl line was improved for all the detectors. In particular, between 0.2 and 0.5 keV were gained for the coaxial detectors, and about 0.15 for the BEGe's (see Tab. 1). In one specific case (Achilles), the presence of strong low frequency noise induced a very poor energy resolution with the semi-Gaussian filter, with 3.59 ± 0.03 keV. The problem was solved by the ZAC filter, for which the FWHM is 2.85 ± 0.02 keV, thus much closer to the resolution of the other BEGe's. The ^{208}Tl peak for Achilles spectrum processed with the semi-Gaussian and the ZAC filter is depicted in the right panel of Fig. 6.

Given the very promising results obtained both with GDL and GERDA data, the ZAC filter is being exploited for the reprocessing of all Phase I physics data and will be used for the reconstruction of Phase II energy spectra, too.

5. Summary and Outlook

In this work, a zero-area finite-length cusp digital filter has been applied to the waveforms acquired in some calibrations of GERDA Phase I: this filter has been chosen among many possible ones, because low frequency disturbances, 1/f and series noise were identified as the main contributions to the sub-optimal energy resolution achieved with the standard semi-Gaussian filtering [22]. When dealing with Ge detectors, with intrinsic energy resolution of order of 0.1%, the baseline restoring algorithm is crucial, as well as the proper treatment of the main noise and disturbances sources. Finally the filter parameters (filter characteristic time and charge integration time) have been optimized for each individual detector.

Applying the ZAC filter algorithm, an improvement of the energy resolution (evaluated at the 2.6 MeV gamma-line of ^{208}Tl) of about 8% for the coaxial detector and 5% for the BEGe ones has been achieved. Both the GERDA calibration data sets and the Phase I physics data sets will be reprocessed using the ZAC filter, to improve the energy resolution of the latter.

As published in [3], it is found that the energy resolution at $Q_{\beta\beta}$ of the Physics Data sets, integrated over about 1.5 year of data taking, is about 0.3 keV worse than expected from calibrations: it is our opinion that this could be caused by *artifact* fluctuations of the energy scale, as determined by the weekly calibration (see Fig. 6), and not by real jumps or fluctuation of the gain of the individual detectors and/or front-end

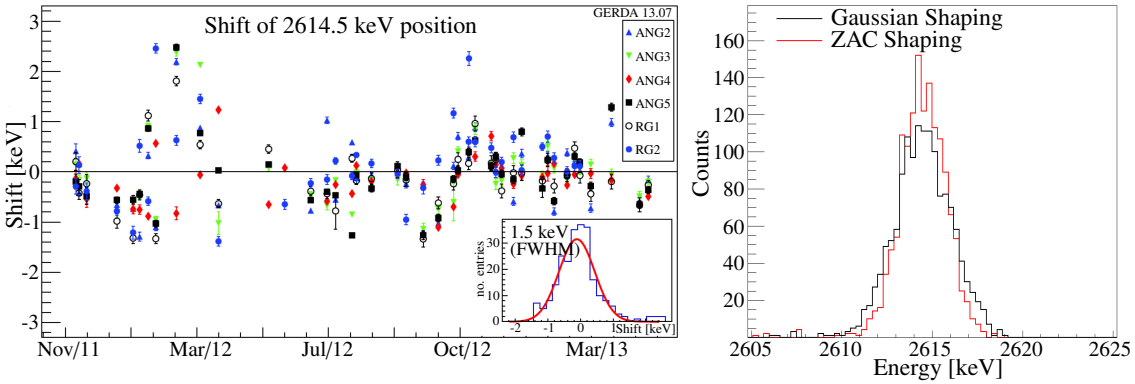

Fig. 6: Left: deviation of the ^{208}Tl peak position as function of time for the coaxial detectors operated in GERDA Phase I, obtained with the semi-Gaussian shaping. Before Juli 2012, a part of the shifts could be explained by cable resistance variations due to temperature instabilities in the clean room. After Juli 2012, the clean room temperature was stabilized within 1°C, therefore shifts of the order of 1 keV are hardly explainable by real jumps or fluctuations of the gain of the detectors and/or the electronics. On the other side, they might be an artifact induced by the semi-Gaussian shaping. Right: ^{208}Tl peak for Achilles, one of the five BEGes used in GERDA Phase I, both for the semi-Gaussian and the ZAC filter, for a typical calibration run. The very poor energy resolution obtained with the semi-Gaussian shaping is due to the presence of low-frequency noise, strongly suppressed by the ZAC filter.

electronics, operated in a close to perfect thermostated environment of 64 m^3 of LAr, or of FADC, operated in thermostated cabinet.

References

[1] K.-H. Ackermann et al. (GERDA Collaboration), The GERDA Experiment for the search of $0\nu\beta\beta$ decay in ^{76}Ge, *Eur. Phys. J.* C73 (2013) 2330.

[2] V. I. Tretyak, False Starts in History of Searches for 2β Decay, or Discoverless Double Beta Decay, *AIP Conf. Proc.* 1417 (2011) 129.

[3] M. Agostini et al. (GERDA Collaboration), Results on neutrinoless double beta decay of ^{76}Ge from GERDA Phase I, *Phys. Rev. Lett.* 111 (2013) 122503.

[4] J. B. Albert et al (EXO Collaboration), Search for Majorana neutrinos with the first two years of EXO-200 data, arXiv:1402:6956v1.

[5] A. Gando et al. (KamLAND-Zen Collaboration), Limit on Neutrinoless $\beta\beta$ Decay of ^{136}Xe from the First Phase of KamLAND-Zen and Comparison with the Positive Claimin ^{76}Ge, *Phys. Rev. Lett.* 110 (2013) 062502.

[6] M. Gunther et al., Heidelberg-Moskow beta beta experiment with Ge-76: Full setup with five detectors, *Phys. Rev. D* 55 (1997) 54-67.

[7] C. E. Aalseth et al., Recent results from the IGEX double-beta decay experiment, *Nucl. Phys. Proc. Suppl.* 48 (1996) 223-225.

[8] Canberra Oak Ridge, USA, and Canberra Semiconductor, NV, Lammerdries 25, B-2250, Olen, Belgium; www.canberra.com.

[9] E. Andreotti et al., HEROICA: an underground facility for the fast screening of germanium detectors, *JINST* 8 (2013) P06012.

[10] M. Agostini et al., GELATIO: a general framework for modular digital analysis of high-purity Ge detector signals, *JINST* 6, P08013 (2011).

[11] S. Riboldi, C. Cattadori, V. D'Andrea and G. Benato, Digital signal processing techniques for HPGe detectors operation, *to be published in IEEE 2013 NSS/MIC/RTSD Conference Record*.

[12] M. O. Deighton, Minimum-noise filters with good low-frequency rejection, *IEEE Trans. Nucl. Sci.*, 16 (1969) 68-75.

[13] R. Abbiati et al., A New Filter Concept Yielding Improved Resolution and Throughput in Radiation Detection Systems, *IEEE Trans. Nucl. Sci.* 52 (2005) 950-953.

[14] V. D'Andrea, *Analisi delle prestazioni di rivelatori Broad Energy Germanium (BEGe) nei test della fase II dell'esperimento GERDA ai LNGS*, Master thesis, University of L'Aquila, 2013, pag. 123-128.

[15] F. S. Goulding and D. A. Landis, Ballistic deficit correction in semiconductor detector spectrometers, *IEEE Trans. Nucl. Sci.* 35 (1988) 119-124.

[16] V. Radeka, Trapezoidal filtering of signals from large germanium detectors at high rates, *NIM* 99 (1972) 525-539.

[17] A. Geraci et al., Automatic Pole-Zero/Zero-Pole Digital Compensator for High-Resolution Spectroscopy: Design and Experiments, *IEEE Trans. Nucl. Sci.* 46 (1999) 817-821.

[18] G. Bertuccio et al., Minimum noise design of fast bipolar integrated amplifiers with low-power constraint, *NIM* A409 (1998) 286-290.

[19] M. Tarka, *Studies of the neutron flux suppression from a γ ray source and the* GERDA *calibration system*, PhD thesis, University of Zurich, 2012.
[20] F. Froborg, Monte Carlo studies and optimization for the calibration system of the GERDA experiment, *NIM* A729 (2013) 557-564.
[21] M. Agostini et al., LArGe R&D for active background suppression in GERDA, *J. Phys.: Conf. Ser.* 375 (2012) 042009.
[22] M. Agostini et al (GERDA Collaboration), The background in the neutrinoless double beta decay experiment GERDA, accepted for publication in *EPJ C*, arXiv:1306.5084.